

2D Simulations of Current-voltage Characteristics of Cubic $\text{Al}_x\text{Ga}_{1-x}\text{N}/\text{GaN}$ Modulation Doped Hetero-junction Field Effect Transistor Structures

Driss Bouguenna^{1,*}, A. Boudghene Stambouli², A. Zado³, D. J. As³, N. Mekkakia Maaza²

¹Department of L.M.D SM, Faculty of Sciences & Technology, University of Mascara, 29000, Mascara, Algeria

²Electrical Engineering Laboratory of Oran, Department of Electronics, Faculty of Electrical & Electronics Engineering, University of Sciences & Technology of Oran, 31000, Oran, Algeria

³Department of Physics, Faculty of Science, University of Paderborn, Warburger Str. 100, 33095 Paderborn, Germany

Abstract We report on calculations of the current-voltage characteristics of cubic $\text{Al}_x\text{Ga}_{1-x}\text{N}/\text{GaN}$ modulation doped hetero-junction field effect transistors using two-dimensional nextnano³ device simulation software. Specifically, we investigate the influence of the thickness and the background doping concentration of cubic GaN buffer on the output and transfer characteristics of the device. Also, the influence of Al content and the effect of a δ -doped layer inserted in the $\text{Al}_x\text{Ga}_{1-x}\text{N}$ are discussed. We find that the maximum saturation current is shown by a structure with a δ -doped layer of $n = 6 \times 10^{18} \text{ cm}^{-3}$, Al content of $x = 25\%$ and a GaN buffer layer thickness of 100 nm. For this structure, our calculations show a low threshold voltage value and the highest transconductance g_m among the sample structure that we used for our calculations.

Keywords Cubic $\text{Al}_x\text{Ga}_{1-x}\text{N}/\text{GaN}$, MODFET, δ -doping, Drain Current, Threshold Voltage, Nextnano³

1. Introduction

The reduction of dimensions in electronic devices such as high electron mobility transistors may allow higher transfer rates in data communication systems[1]. $\text{Al}_x\text{Ga}_{1-x}\text{N}/\text{GaN}$ based high electron mobility transistors (HEMT) have shown great potential for high-frequency and high-power applications. In fact, $\text{Al}_x\text{Ga}_{1-x}\text{N}/\text{GaN}$ HEMTs exploit the advantages of the wide band gap GaN materials, namely high mobility and high carriers density reached by the two dimensional electron gas (2DEG) formed at the hetero-interface[2]. This is motivated by their potential in commercial and military applications, e.g., in the area of telecommunication systems, base stations market, as well as radar, W-CDMA mobile-phone applications[3],[4], high temperature electronics, high power solid state switching, and hard radiation in space electronics.

However, the cubic nitrides would allow using the same technology for normally-on and normally-off devices[5]. So far, the important problem is transconductance (g_m) decrease due to a large parasitic resistance[6],[7] in normally-off MODFETs devices, and shows result of large

gate leakage current and current collapse, which is mainly due to the cubic $\text{Al}_x\text{Ga}_{1-x}\text{N}$ surface under the gate. The development of these devices, is still hindered by some problems including large gate leakage current[8],[9] drain current collapse[10] at high frequencies, and poor long-term reliabilities of the Schottky gate. Large gate leakage affects the device's noise level, especially at elevated temperature when gate leakage increases significantly[11] whichever with some problems including gate leakage, current collapse, reliability, and yield.

In addition, cubic $\text{Al}_x\text{Ga}_{1-x}\text{N}/\text{GaN}$ MODFETs with normally-on and normally-off output and transfer characteristics depending on the doping concentration, the thickness of the buffer layer and Al content of the $\text{Al}_x\text{Ga}_{1-x}\text{N}$ barrier were demonstrated. The devices are simulated by I-V characteristics using two-dimensional nextnano³ device simulation software. The sample structures for improved cubic $\text{Al}_x\text{Ga}_{1-x}\text{N}/\text{GaN}$ MODFET devices were developed. In this paper a direct methodology to investigate the influence of the thickness and the background doping concentration of cubic GaN buffer on the I-V characteristics of the device. Also, the influence of Al content and the effect of a δ -doped layer inserted in the $\text{Al}_x\text{Ga}_{1-x}\text{N}$ are discussed. Our device exhibits maximum drain source saturation current of $I_{DSsat} = 130 \text{ A/m}$ for $x = 25\%$ and clear field-effect at positive bias voltages with threshold voltage of $V_{th} = 0.4 \text{ V}$ compared with the results similar which obtained by Saint Martin et al, for double gate MOSFETs[12].

* Corresponding author:

dbouguenna29@gmail.com (Driss Bouguenna)

Published online at <http://journal.sapub.org/eee>

Copyright © 2012 Scientific & Academic Publishing. All Rights Reserved

2. Basics of HEMTs

The unique feature of HEMT device is the hetero-structure interface where a two dimensional electron gas channel is formed. Also due to this modulation doping, carriers diffuse into the undoped hetero-interface[13]. To avoid impurity scattering, the carriers are spatially separated from the doped region using a thin (1 - 5) nm $\text{Al}_x\text{Ga}_{1-x}\text{N}$ spacer layer. The idea of the modulation doped structure was proposed at Bell Laboratories in the late 1970s[13] and then in 1978, Dingle et al. first demonstrated enhanced mobility in the $\text{Al}_x\text{Ga}_{1-x}\text{As}/\text{GaAs}$ modulation doped super-lattice structure[14]. In 1979 Stormer et al. subsequently reported similar effect using a single $\text{Al}_x\text{Ga}_{1-x}\text{As}/\text{GaAs}$ hetero-junction[15]. These studies were made on two-terminal devices without the control gate. This effect was applied to the field-effect transistor by Mimura et al. in 1980[16],[17] and later by Delagebeaudeuf et al. in the same year[18]. Since then, the HEMT has been the topic of major research activities and has matured to commercial products as an alternative to MESFETs in high-speed circuits[19-22]. However, these basic characteristics of $\text{Al}_x\text{Ga}_{1-x}\text{As}/\text{GaAs}$ HEMTs are also essentials to $\text{Al}_x\text{Ga}_{1-x}\text{N}/\text{GaN}$ modulation doped hetero-junction field effect transistors (MODFETs) in order to understand their bases.

The main advantage of modulation doping is the elimination of traps in the $\text{Al}_x\text{Ga}_{1-x}\text{N}$ layer and of the parallel conduction path within this doped $\text{Al}_x\text{Ga}_{1-x}\text{N}$ layer. This is due to decreased parasitic channel in the $\text{Al}_x\text{Ga}_{1-x}\text{N}$ layer. Thereby, the mobility of transistors is superior. The bulk mobility as a function of temperature shows a peak at a certain temperature. The decrease of bulk mobility with increase of temperature is due to phonon scattering. At low temperatures, the bulk mobility is limited by impurity scattering. It depends, as expected, on the doping level and it also decreases with a decrease of temperature. In the modulation-doped channel, mobility at temperatures above ≈ 80 K is comparable to the value of a low doped bulk sample. However, mobility is much enhanced at lower temperatures[23].

2.1. Basic Device Structure

A basic MODFET structure based on the $\text{Al}_x\text{Ga}_{1-x}\text{N}/\text{GaN}$ system is shown in Figure 1. It can be noted that the barrier $\text{Al}_x\text{Ga}_{1-x}\text{N}$ layer under the gate is doped, while the GaN buffer layer is undoped. The doped barrier layer is typically around 20 nm thick. Very often, instead of uniform doping, a δ -doped charge sheet is used within the barrier layer and placed close to the channel interface. The source and drain contacts are ohmic, while the gate is a Schottky barrier. Sometimes, the top layer of n^+ -GaN on $\text{Al}_x\text{Ga}_{1-x}\text{N}$ is used for better source and drain ohmic contacts. The deeper n^+ -regions of source/drain are formed either by ion implantation or introduced during the alloying step to contact the electron channel. For low values of drain-to-source bias, the current flows from drain-to-source

through the electron channel. The carrier sheet density and consequently the conductivity of the channel are controlled by the gate bias. Increasing of the positive bias applied to the gate increases the depth of the potential well at the $\text{Al}_x\text{Ga}_{1-x}\text{N}/\text{GaN}$ interface. This results in enhanced sheet carrier density of the electron channel, therefore increasing current conduction. On the contrary, increasing of the negative gate bias decreases the depth of the electron channel and the sheet carrier density decreases, thereby lowering the channel conductivity.

In the device geometry, the most-important parameter is the gate length L_G . This dimension determines the maximum frequency limits for MODFET devices. Typical gate lengths are in the 0.1... 2 μm range. The gate width Z is another physical device dimension that is of primary importance to the determination of device behavior. The device current is directly proportional to the gate width because of the cross section area, available for the channel current, is proportional to Z . For low noise and low current applications, devices with relatively small gate width are utilized. In contrast, large gate width devices are typically used for power applications. Other characteristic dimensions are: the gate-to-source L_{GS} , gate-to-drain L_{GD} spacing, the drain L_D and source length L_S .

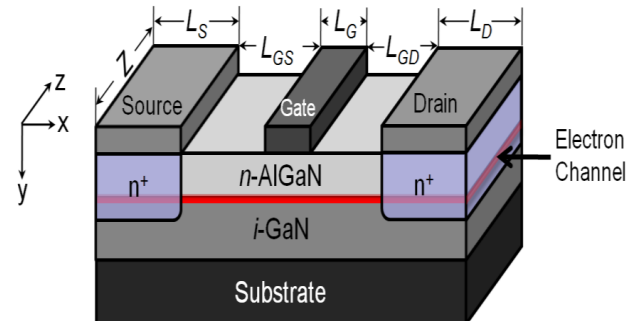


Figure 1. Typical structure of MODFET using the basic $\text{Al}_x\text{Ga}_{1-x}\text{N}/\text{GaN}$ system

2.2. Current-Voltage Characteristics

In this work, n -channel devices based on cubic $\text{Al}_x\text{Ga}_{1-x}\text{N}/\text{GaN}$ with a two dimensional channel formed by electrons were calculated. There are two different types of FETs depending on the state of the transistors with zero gate bias. Their schematic output and transfer characteristics are shown in Figure 2. The energy band diagrams at equilibrium (calculated for a cubic $\text{Al}_x\text{Ga}_{1-x}\text{N}/\text{GaN}$ hetero-structure) are illustrated in Figure 3. FETs are called enhancement-mode or normally-off if at zero bias the channel is depleted and the Fermi level E_F is below the conduction band edge E_C . In this mode the conduction of the electron channel is very low and a positive gate voltage must be applied to populate the channel with carriers. The counterpart is called depletion mode, or normally-on, if the channel is conductive for zero gate bias. The Fermi level E_F crosses the conduction band edge at the $\text{Al}_x\text{Ga}_{1-x}\text{N}/\text{GaN}$ hetero-interface. Negative gate voltage must be applied to turn the transistor-off.

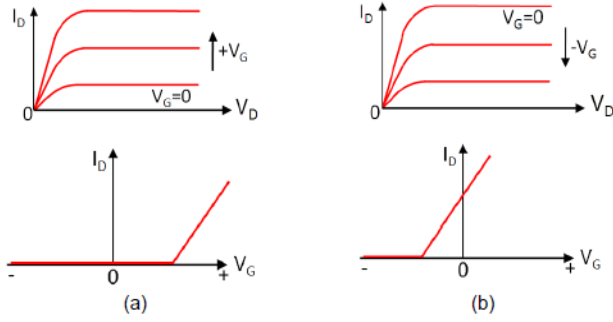


Figure 2. Comparison of current-voltage characteristics, for (a) normally-on (depletion-mode) FET and (b) normally-off (enhancement-mode) FET

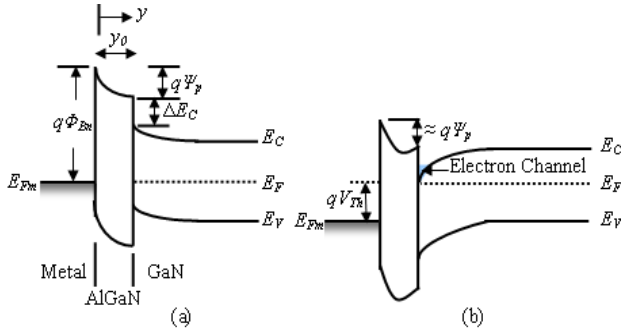


Figure 3. Room temperature energy-band diagrams for a normally-off MODFET at (a) equilibrium and (b) onset of threshold

Based on the principle of modulation doping, the impurities within the barrier layer are completely ionized and carriers depleted away. Referring to the energy-band diagrams of Figure 3, the pinch-off voltage for $\text{Al}_x\text{Ga}_{1-x}\text{N}$ layer V_p within the depletion region is given by:

$$V_p = -\frac{q}{\epsilon_s} \int_0^{y_0} N_D(y) y dy \quad (1)$$

for a general doping profile. However, for uniform doping this built-in potential becomes:

$$V_p = \frac{qN_D y_0^2}{2\epsilon_s} \quad (2)$$

where q is the magnitude of the electronic charge, N_D is the donor impurity concentration within the barrier layer and ϵ_s is the dielectric permittivity of the semiconductor.

The threshold voltage is the gate bias at which the channel starts to form between the source and drain. It is the voltage around which the transistor is turned on and off and is the most important parameter for the FET device. As can be seen in Figure 3 (b), when the Fermi level E_F at the GaN surface coincides with conduction band edge E_C the threshold voltage is given by:

$$V_{th} \approx \phi_{Bn} - V_p - \frac{\Delta E_C}{q} \quad (3)$$

By choosing the doping profile and the barrier height ϕ_{Bn} , V_{th} can be varied between positive and negative values. An example for a positive threshold voltage V_{th} is shown in Figure 4 and the transistor shows normally-off characteristics. Moreover, with a gate voltage larger than

the threshold voltage the 2DEG sheet in the channel induced by the gate as a function of the distance x is capacitive coupled and is given by:

$$n_s(x) = \frac{C_0[V_G - V_{th} - \psi(x)]}{q} \quad (4)$$

where

$$C_0 = \frac{\epsilon_s}{y_0 + y_{UID} + \Delta y} \quad (5)$$

y_0 and y_{UID} are the doped and undoped $\text{Al}_x\text{Ga}_{1-x}\text{N}$ thickness and Δy is the channel thickness of the two-dimensional electron gas, estimated to be around (8 - 10) nm. $\psi(x)$ is the channel potential with respect the source and (x is the direction from drain-to-source). It varies along the channel from zero to the drain bias V_D . The drift current at any point along the channel is given by:

$$\begin{aligned} I_{DS}(x) &= W\mu_n q n_s E(x) \\ &= W\mu_n C_0 [V_G - V_{th} - \psi(x)] \frac{d\psi(x)}{dx} \end{aligned} \quad (6)$$

where W is the depletion width and μ_n is the drift mobility of electron.

Since the current is constant throughout the channel, integrating the above equation from source-to-drain gives:

$$I_{DS} = \frac{W\mu_n C_0}{L} \left[(V_G - V_{th})V_{DS} - \frac{V_{DS}^2}{2} \right] \quad (7)$$

The output characteristics for an enhancement-mode MODFET are shown in Figure 4. In the linear region where $V_{DS} \ll (V_G - V_{th})$, Eq. (7) is reduced to an ohmic expression:

$$I_{lin} = \frac{W\mu_n C_0 (V_G - V_{th}) V_{DS}}{L} \quad (8)$$

from the equation (8), the transconductance can be obtained as follow:

$$g_{m,lin} \equiv \frac{dI_{lin}}{dV_G} = \frac{W\mu_n C_0 V_{DS}}{L} \quad (9)$$

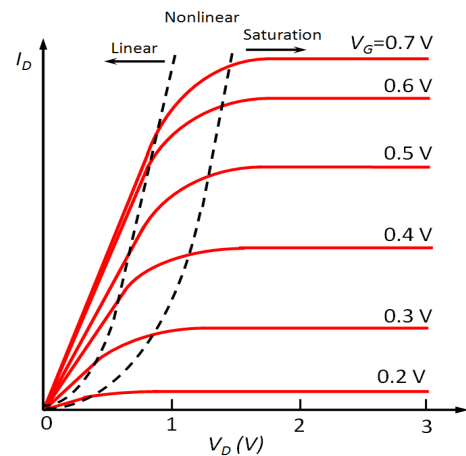


Figure 4. Output characteristics of an enhancement-mode MODFET

At high V_{DS} , n_s at the drain is reduced to zero, corresponding to the pinch-off condition and current saturates with V_{DS} . It can be shown from Eq. (4) that:

$$V_{DS,sat} = V_G - V_{th} \quad (10)$$

and this gives a drain current saturation of:

$$I_{DS,sat} = \frac{W\mu_n C_0}{2L} (V_G - V_{th})^2 \quad (11)$$

The transconductance becomes:

$$g_{m,sat} \equiv \frac{dI_{sat}}{dV_G} = \frac{W\mu_n C (V_G - V_{th})}{L} \quad (12)$$

For a uniform doped layer and changing y_0 , the threshold voltage V_{th} can have a positive or negative value. Therefore, if V_{th} is positive the transistor is called an enhancement-mode (normally-off) and in negative case, a depletion-mode (normally-on)[24].

3. Results and Discussion

3.1. Variation in Thickness of Cubic GaN Buffer Layer

In our calculations we use 3C-SiC (001) as the substrate for the cubic $\text{Al}_x\text{Ga}_{1-x}\text{N}/\text{GaN}$ MODFET structures. Figure 5 shows a schematic drawing of the structure of MODFETs (sample A). The thickness of the UID c-GaN buffer layer was varied in the calculations. The background n -type doping concentration in this layer is $N_D = 1 \times 10^{17} \text{ cm}^{-3}$. On top of GaN buffer a 4 nm UID cubic $\text{Al}_{0.25}\text{Ga}_{0.75}\text{N}$ spacer layer with $N_D = 4 \times 10^{17} \text{ cm}^{-3}$, 6 nm cubic $\text{Al}_{0.25}\text{Ga}_{0.75}\text{N}:\text{Si}$ with $N_D = 4 \times 10^{18} \text{ cm}^{-3}$ and 10 nm UID cubic $\text{Al}_{0.25}\text{Ga}_{0.75}\text{N}$ with $N_D = 4 \times 10^{17} \text{ cm}^{-3}$ are placed. In addition, we use two-dimensional device simulator *nextnano*³ software[25] for numerical simulation of the electrical output and transfer characteristics. Our devices have a gate length of $2 \mu\text{m}$ and a source-to-drain spacing of $8 \mu\text{m}$.

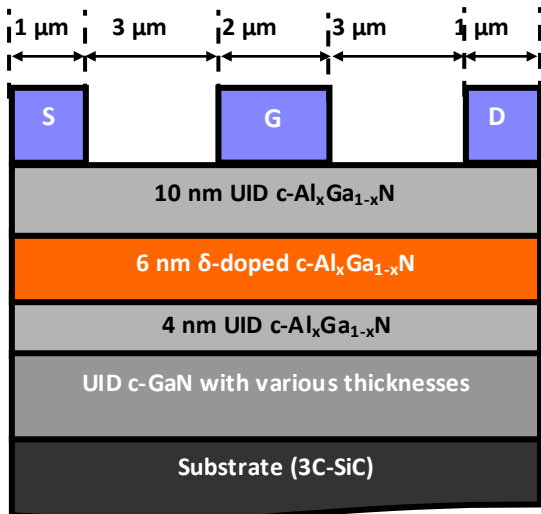


Figure 5. Cross sectional view of cubic $\text{Al}_x\text{Ga}_{1-x}\text{N}/\text{GaN}$ based MODFETs (sample A) using for simulation

Figure 6 shows the calculated output characteristics of cubic $\text{Al}_x\text{Ga}_{1-x}\text{N}/\text{GaN}$ MODFETs. From the calculations we obtain an increase of the drain-to-source current with the decreasing of the thickness of the cubic GaN buffer layer is obtained by the calculation. However, the drain-to-source

current at $V_G = 0 \text{ V}$ is relatively large due to the high conductivity of 100 nm thickness of cubic GaN buffer layer. The transfer characteristics of the transistor at $V_{DS} = 0 \text{ V}$ are shown in Figure 7. According to the calculated curves, we can achieve a high electrons sheet concentration and therewith by reducing impurity scattering, an increase of electron mobility within the channel and a high device transconductance.

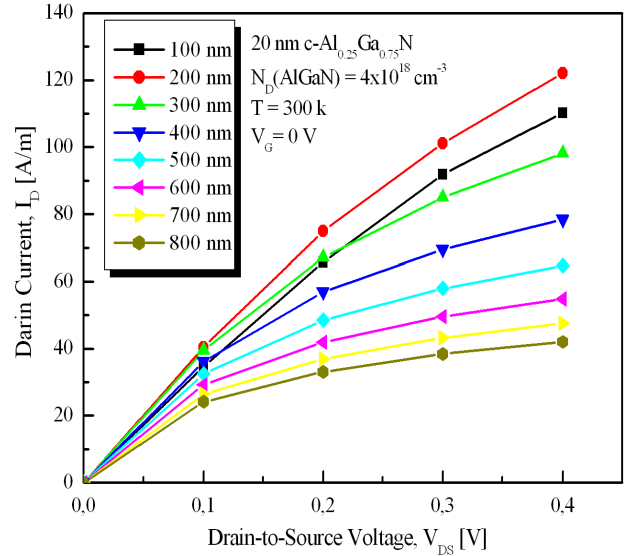


Figure 6. Room temperature electrical output characteristics of cubic $\text{Al}_x\text{Ga}_{1-x}\text{N}/\text{GaN}$ MODFETs (sample A), calculated using *nextnano*³ devices simulation software, for different thickness of c-GaN buffer at $V_{GS} = 0 \text{ V}$

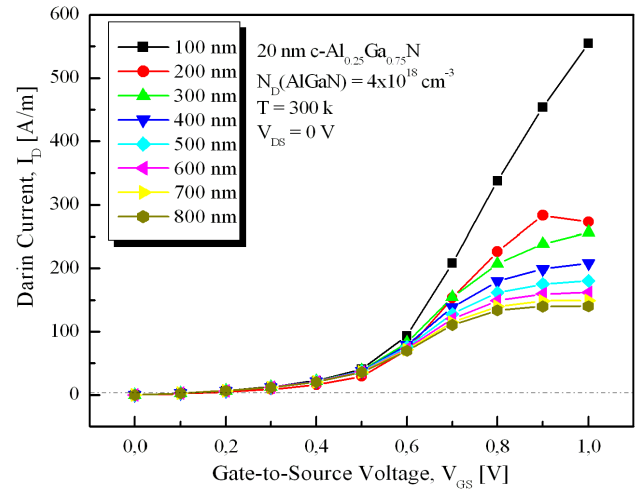


Figure 7. Room temperature transfer characteristics of cubic $\text{Al}_x\text{Ga}_{1-x}\text{N}/\text{GaN}$ MODFETs (sample A), calculated using *nextnano*³ devices simulation software, for different thickness of c-GaN buffer at $V_{DS} = 0 \text{ V}$

3.2. Variation in Donor Concentration Within the δ -doped Layer

Figure 8 shows the structure of sample B consisting of 200 nm unintentionally doped (UID) cubic GaN buffer layer, 4 nm UID cubic $\text{Al}_{0.25}\text{Ga}_{0.75}\text{N}$ spacer layer, 6 nm cubic $\text{Al}_{0.25}\text{Ga}_{0.75}\text{N}:\text{Si}$ and 10 nm UID cubic $\text{Al}_{0.25}\text{Ga}_{0.75}\text{N}$.

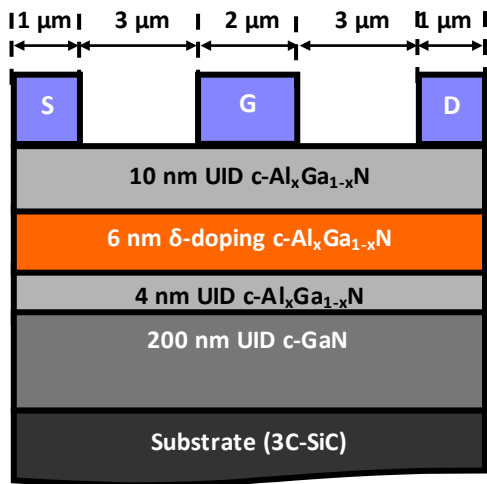


Figure 8. Cross sectional view of cubic $\text{Al}_x\text{Ga}_{1-x}\text{N}/\text{GaN}$ based MODFETs (sample B) using for simulations

For the effects of the cubic $\text{Al}_{0.25}\text{Ga}_{0.75}\text{N}$ δ -doping, the maximum transconductance of MODFETs device depends on the maximum carrier sheet density in the channel at the $\text{Al}_x\text{Ga}_{1-x}\text{N}/\text{GaN}$ interface. The carriers in the electron channel are generally transferred from $\text{Al}_x\text{Ga}_{1-x}\text{N}$ barrier to the hetero-interface. Therefore, doping of $\text{Al}_x\text{Ga}_{1-x}\text{N}$ barrier is necessary to achieve high electron sheet concentration and therewith high device transconductance. The use of a δ -doped layer within $\text{Al}_x\text{Ga}_{1-x}\text{N}$ barrier placed close to the channel interface allows the local separation of electrons and donors to reduce impurity scattering and increase electron mobility within the channel.

Calculations were performed with the described model to estimate an optimized δ -doping concentration within cubic $\text{Al}_{0.25}\text{Ga}_{0.75}\text{N}$ barrier layer. Figure 9 shows transfer characteristics of cubic $\text{Al}_x\text{Ga}_{1-x}\text{N}/\text{GaN}$ MODFETs for different δ -doping levels. According to the calculated curves, all devices with δ -doped cubic $\text{Al}_x\text{Ga}_{1-x}\text{N}$ layers are fully depleted already at $V_{DS} = 0$ V.

Moreover, the drain-to-source current increases with increasing δ -doping level within the cubic $\text{Al}_{0.25}\text{Ga}_{0.75}\text{N}$ layer, and therewith high device transconductance is achieved. The calculation of the electrical transfer characteristics visualize that intentional doping of cubic $\text{Al}_x\text{Ga}_{1-x}\text{N}$ barrier layer is essential to obtain high device transconductance. With the highest doping concentration of δ -layer, that is $N_D(\delta) = 6 \times 10^{18} \text{ cm}^{-3}$, the device exhibits the highest drain saturation current as shown in Figure 10.

These results show that to accomplish the modulation doping of the barrier layer it is necessary to use a δ -doped layer within $\text{Al}_x\text{Ga}_{1-x}\text{N}$ barrier, placed close to the channel interface, which allows the local separation of electrons and donors. This method allows a reduced impurity scattering and increases the electron mobility within the channel. The Schottky gate contact with a barrier height of 0.8 eV was localized on top of the cubic $\text{Al}_x\text{Ga}_{1-x}\text{N}$ layer. As in the realized MODFET devices [26], the gate length was 2 μm and the gate-to-source and gate-to-drain spacing was 3 μm .

It was not possible to include the effect of gate leakage in the simulation.

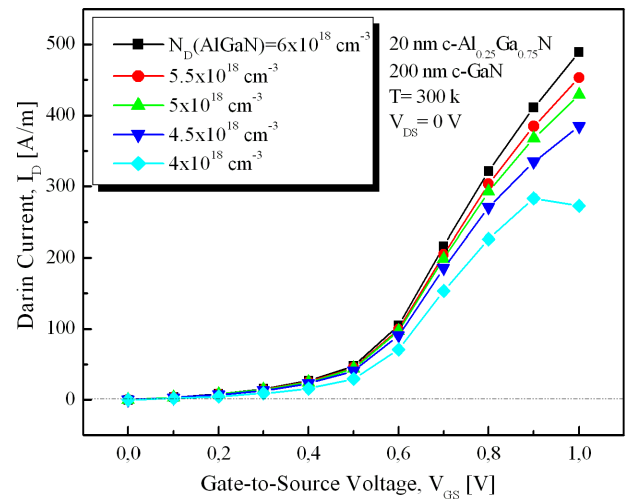


Figure 9. Room temperature transfer characteristics of cubic $\text{Al}_x\text{Ga}_{1-x}\text{N}/\text{GaN}$ MODFETs (sample B), δ -doping level varied within the $\text{Al}_{0.25}\text{Ga}_{0.75}\text{N}$ barrier layer at $V_{DS} = 0$ V

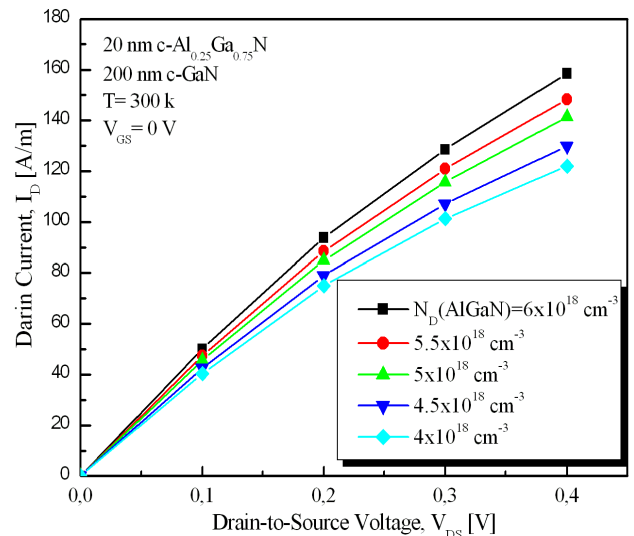


Figure 10. Room temperature output characteristics of cubic $\text{Al}_x\text{Ga}_{1-x}\text{N}/\text{GaN}$ MODFETs (sample B), for different δ -doping $\text{Al}_x\text{Ga}_{1-x}\text{N}$ barrier layer at $V_{GS} = 0$ V

3.3. Simulation at Different Voltages

Figure 11 shows the room temperature dc drain current voltage (I-V) curves of a cubic MODFETs device. A clear field-effect was calculated with this device when the gate-to-source voltage varied from -100 mV to +100 mV. The increase in the calculated drain current with increasing V_G proves a good agreement with the normally-off MODFET devices. However, it is possible to include the effect of gate leakage in the simulations.

Furthermore, the transfer characteristics of cubic MODFETs (sample B) were calculated with the two-dimensional device simulator nextnano³, for different drain-to-source voltages from -100 mV to +100 mV and are displayed in Figure 12. The threshold voltage of this device

is +0.4 V at $V_{DS} = 0$ V. This indicates normally-off device characteristics.

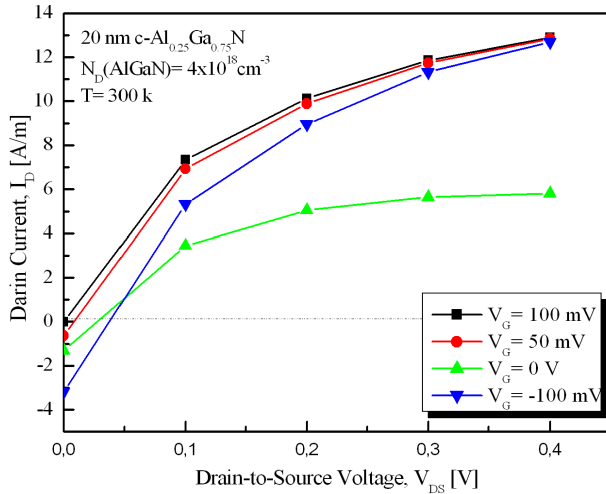


Figure 11. Room temperature output characteristics of cubic $\text{Al}_x\text{Ga}_{1-x}\text{N}/\text{GaN}$ MODFET sample B, calculated using *nextnano*³ devices simulation software at $V_G = -0.1$ V, 0 V, +50 mV, and +0.1 V

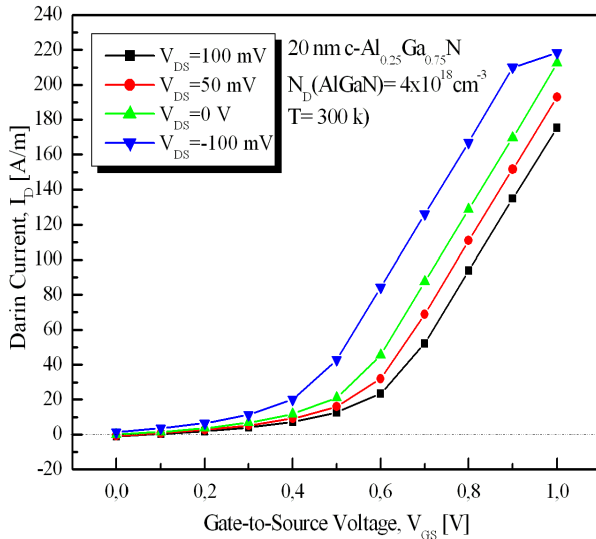


Figure 12. Room temperature transfer characteristics of cubic $\text{Al}_x\text{Ga}_{1-x}\text{N}/\text{GaN}$ MODFETs (sample B), calculated using *nextnano*³ devices simulation software at $V_{DS} = -0.1$ V, 0 V, +50 mV, and +0.1 V

3.4. Variation in Al Content within the $\text{Al}_x\text{Ga}_{1-x}\text{N}$ barrier Layer

Figure 13 shows calculations of the electrical output characteristics of a MODFET transistor, for different Al content x in the $\text{Al}_x\text{Ga}_{1-x}\text{N}$ barrier layer. Our results show that, for $x = 25\%$ the MODFET reaches the maximum drain source saturation current of $I_{DSsat} = 130$ A/m compared with those obtained with $x = 30\%$, 32% and 33% . The electrical transfer characteristics are shown in Figure 14, where the MODFET presents a low threshold voltage around 0.4 V for Al content $x = 25\%$. The electrical output and transfer characteristics were calculated at $V_{GS} = 0$ V and $V_{DS} = 0$ V respectively. Results show that an improvement of the device transconductance and of the performance of

normally-off MODFET devices can be reached by varying Al content in the $\text{Al}_x\text{Ga}_{1-x}\text{N}$ barrier layer.

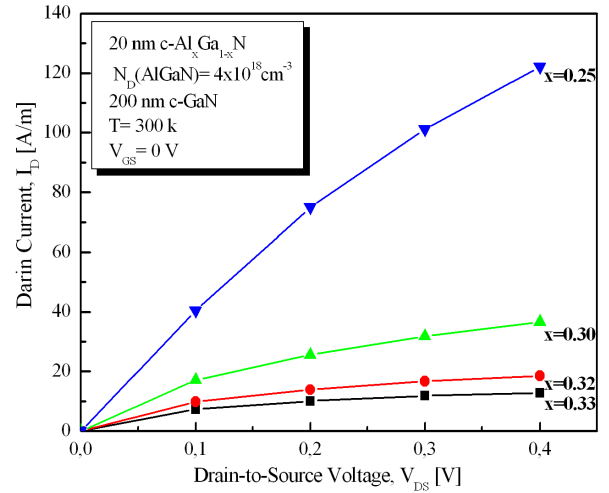


Figure 13. Room temperature electrical output characteristics of cubic $\text{Al}_x\text{Ga}_{1-x}\text{N}/\text{GaN}$ MODFETs (sample B), calculated using *nextnano*³ devices simulation software, for different Al contents

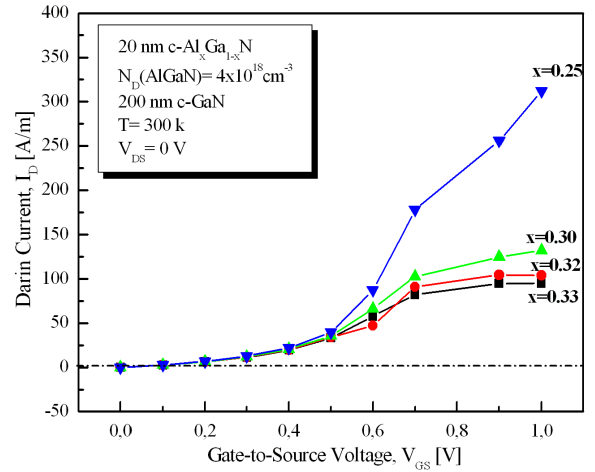


Figure 14. Room temperature electrical transfer characteristics of cubic $\text{Al}_x\text{Ga}_{1-x}\text{N}/\text{GaN}$ MODFETs (sample B), calculated using *nextnano*³ devices simulation software, for different Al contents

4. Conclusions

The main focus of this work is the simulations results of the output and transfer characteristics of cubic $\text{Al}_x\text{Ga}_{1-x}\text{N}/\text{GaN}$ based MODFETs structures, by using samples with a different thickness of cubic GaN buffer layer and with different δ -doping and different Al contents. Our results show a clear field-effect at positive bias voltages with $V_{th} = 0.4$ V. However, due to the gate leakage the device has not yet exhibited the characteristics of an ideal normally-off FET. On one hand, our results of simulations demonstrate clearly that cubic $\text{Al}_{0.25}\text{Ga}_{0.75}\text{N}/\text{GaN}$ can be used for the MODFETs with normally-off mode operation behavior. On the other hand, simulation of the output characteristics is in good agreement

with the finding that the shunt current is mainly due to the gate leakage. In addition, we find the highest values of drain source saturation current for a device with 100 nm of buffer layer, $N_D(\delta) = 5.5 \times 10^{18} \text{ cm}^{-3}$ or around $N_D(\delta) = 6 \times 10^{18} \text{ cm}^{-3}$, and Al content of the barrier layer $x = 25\%$, at $V_{GS} = 100 \text{ mV}$. For this structure, the transfer characteristics show a low threshold voltage value and the highest maximum transconductance g_m , among the simulated MODFET structures.

ACKNOWLEDGMENTS

The work is a joint collaboration between the group of Physics and Technology of Optoelectronic Semiconductors at University of Paderborn, Germany and Laboratory of Electrical Engineering at University of Sciences and Technology of Oran, Algeria.

REFERENCES

- [1] J. Schörmann, S. Potthast, D.J. As, K. Lischka, "Near UV Emission from Non-polar Cubic $\text{Al}_x\text{Ga}_{1-x}\text{N}/\text{GaN}$ Quantum Wells", *Appl. Phys. Lett.* 89, 131910, 2006.
- [2] H. Morkoç, A. Di Carlo, R. Cingolani, "GaN-based Modulation Doped FETs and UV Detectors", *Solid-State Electronics* 46, pp.157-202, 2002.
- [3] M. Abe, "A Quarter Century of HFET Device Technology", *Univ. of Hosei, Proc.21st Symposium on Materials Science and Engineering, Research Center of Ion Beam Technology*, pp. 7-14, Dec 2002.
- [4] K. Joshin, T. Kikkawa, H. Hayashi, T. Maniwa, S. Yokokawa, M. Yokoyama, N. Adachi, M. Takikawa, "A 174 W High-Efficiency GaN HFET Power Amplifier for W-CDMA Base Station Application", *IEEE IED: Tech, Digest*, pp. 983-985, Dec 2003.
- [5] E. Tschumak, R. Granzner, J. K. N. Lindner, F. Schwierz, K. Lischka, H. Nagasawa, M. Abe, D.J. As, "Non-polar Cubic $\text{Al}_x\text{Ga}_{1-x}\text{N}/\text{GaN}$ Hetero-Junction Field Effect Transistor on Ar^+ Implanted 3C-SiC (001)", *Appl. Phys. Lett.*, vol. 96, 253501, June 2010.
- [6] T. Palacios, C.S. Suh, A. Chakraborty, S. Keller, S.P. DenBaars, U. K. Mishra, "High Performance E-mode AlGaIn/GaN HEMTs", *IEEE Electron Device Lett.*, vol. 27, no.6, pp. 428-430, June 2006.
- [7] Y. Cai, Y. Zhou, K.M. Lau, and k.J. Chen, "High Performance Enhancement-Mode $\text{Al}_x\text{Ga}_{1-x}\text{N}/\text{GaN}$ HFETs using Fluoride Based Plasma Treatment", *IEEE Trans, Electron devices*, vol. 53, no. 9, pp. 2207-2215, Sep 2006.
- [8] M.A. Khan, X. Hu, A. Tarakji, G. Simin, J. Yang, *Appl. Phys. Lett.* 77, 1339, 2000.
- [9] E.J. Miller, X.Z. Dang, and E.T. Yu, *J. Appl. Phys.* 88, 5951, 2000.
- [10] R. Vetury, N.Q. Zhang, S. Keller, U.K. Mishra, *IEEE Trans, Electron Devices* 48, 560, 2001.
- [11] X. Hu, A. Koudymov, G. Simin, J. Yang, M.A. Khan, A. Tarakji, M.S. Shur, R. Gaska, *Appl. Phys. Lett.* 79, 2832, 2001.
- [12] J.S. Martin, A. Bournal, P. Dollfus, "On the Ballistic Transport in Nanometer Scaled Double Gate MOSFET", *University of Paris South, Institute of Electronic Fundamental, CNRS UMR 8622, Buil. 220*, 2003.
- [13] F. Sacconi, A. Di Carlo, P. Lugli, H. Morkoc, "I Spontaneous and Piezoelectric Polarization Effects on the Output Characteristics of $\text{Al}_x\text{Ga}_{1-x}\text{N}/\text{GaN}$ Hetero-Junction Modulation Doped FETs", *IEEE Transaction on Electron Devices*, vol. 48, no.3, pp. 586-590, March 2001.
- [14] R. Dingle, H. L. Stormer, A. C. Gossard, and W. Wiegmann, "Electron Mobilities in Modulation Doped Semiconductor Heterojunction Superlattices", *Appl. Phys. Lett.*, 33, 665, 1978.
- [15] H. L. Stormer, R. Dingle, A.C. Gossard, W. Wiegmann, and M. D. Sturge, "Two-Dimensional Electron Gas at a Semiconductor-Semiconductor Interface", *Solid State Commun.*, 29, 705, 1979.
- [16] T. Mimura, S. Hiyamizu, T. Fujii, and K. Nanbu, "A New Field-Effect Transistor with Selectively Doped $\text{GaAs}/\text{n-Al}_x\text{Ga}_{1-x}\text{As}$ Heterojunctions", *Jpn. J. Appl. Phys.*, vol.19, pp. 225-227, 1980.
- [17] T. Mimura, "The Early History of the High Electron Mobility Transistor (HEMT)", *IEEE Trans. Microwave Theory Tech.*, vol. 50, no.3, pp. 780-782, 2002.
- [18] D. Delagebeaudeuf, P. Delescluse, P. Etienne, M. Laviron, J. Chaplart, and N. T. Linh, "Two-Dimensional Electron Gas MESFET Structure", *Electronics Letters*, vol.16, no.17, 15th, pp. 667-668, August 1980.
- [19] H. Daembkes, Ed., "Modulation Doped Field-Effect Transistors: Principle, Design and Technology", *IEEE Press, Piscataway, New Jersey*, 1991.
- [20] H. Morkoc, H. Unlu, and G. Ji, "Principles and Technology of MODFET: Principles, Design and Technology", vols. 1 and 2, *Wiley, New York*, 1991.
- [21] C. Y. Chang and F. Kai, "GaAs High-Speed Devices", *Wiley, New York*, 1994.
- [22] M. Golio and D.M. Kingsriter, Eds, "RF and Microwave Semiconductor Devices Handbook", *CRC Press, Boca Raton, Florida*, 2002.
- [23] S.M. Sze, K.K. Ng "Physics of Semiconductors Devices", Third Ed., *Wiley-Inter-Science*, 2007.
- [24] S.M. Sze, "Modern Semiconductor Device Physics", *John Wiley & Sons, Inc*, 1998.
- [25] Online Available: [http://www.wsi.tum.de/nextnano³](http://www.wsi.tum.de/nextnano3) and <http://www.nextnano.de>.
- [26] D.J. As, E. Tschumak, I. Laubenstein, R.M. Kemper, K. Lischka, "Schottky and Ohmic Contacts on Non-polar Cubic GaN Epilayers", *MRS Symposium Proceedings*, 1108, A01-02, 2009.